of ε the values of λ deviate only slightly from those for the Darcy case. As ε increases, these curves approach the line $1+\varepsilon\lambda = 0$ which corresponds to singular points of equations (11) and (12). This critical line arises because the time-dependent term introduced into the Darcy equations causes the term with the highest order spatial derivative to have a coefficient which varies and which is zero on the critical line if λ is real. In this sense the present problem is similar to the inviscid Orr–Sommerfeld problem. Here, however, one has no need to resort to a critical layer analysis as λ becomes complex in order to pass 'around' the critical line.

On fixing S and α, there are only two possible ways for λ (for the most unstable mode) to evolve as ε increases: either λ asymptotes to the curve $\varepsilon\lambda$ = negative constant, or two stationary modes ($\mathrm{Im}(\lambda) = 0$) coalesce to form a pair of travelling modes ($\mathrm{Im}(\lambda) \neq 0$), which can then pass around the critical line, followed by a decoupling of the modes which both eventually asymptote to λ = constant. The former possibility is not evident in Fig. 3 and therefore, for a clearer representation, one rescales the ordinate by plotting $-\varepsilon\,\mathrm{Re}(\lambda)$. On using a log–log scaling, both asymptotic forms are shown as straight lines, the former having unit slope and the latter being horizontal as is the critical line. These may be seen clearly in Fig. 4.

In Fig. 4 the decrement spectrum is displayed for the three cases, $\alpha = 0.25\pi$, $S = 10$, 50 and 200. These figures are typical of all those calculated for different values of α and S. It is a universal feature of the results that when ε is small the effect of increasing either α, S or both is to decrease $\mathrm{Re}(\lambda)$ still further, at least for the most unstable mode; this is similar to the Darcy case as shown in Fig. 2. As ε increases the slope of $\ln(-\varepsilon\,\mathrm{Re}(\lambda))$ for the most unstable mode usually remains positive and $\mathrm{Re}(\lambda)$ is always negative.

To conclude, one has demonstrated that non-zero values of the inverse Prandtl–Darcy number do not induce instabilities of the form of rolls of any orientation. This is also true for unphysically large values of ε. The question which immediately arises is to ask why the results are at variance with those of Georgiadis and Catton [6], who gave an expression for the critical Grashof number (Gr_{crit}; equivalent to our critical Rayleigh number) for instability. A careful examination of that expression and the preceding analysis shows that the defining integrals for Gr_{crit} contain the Grashof number itself, and therefore their expression defines the critical Grashof number implicitly. The results indicate that such a value does not exist and that the flow is linearly stable.

Acknowledgement—The author would like to acknowledge the support of S.E.R.C. during the preparation of this work.

REFERENCES

1. D. S. Riley and D. A. S. Rees, Non-Darcy natural convection from arbitrarily inclined heated surfaces in saturated porous media, *Q. J. Mech. Appl. Math.* **38,** 277–295 (1985).
2. A. Bejan and D. Poulikakos, The non-Darcy regime for vertical boundary layer natural convection in a porous medium, *Int. J. Heat Mass Transfer* **27,** 717–722 (1984).
3. B. Borkowska-Pawlak and W. Kordylewski, Stability of two-dimensional natural convection in a porous layer, *Q. J. Mech. Appl. Math.* **35,** 279–290 (1982).
4. C. T. Hsu and P. Cheng, The Brinkman model for natural convection about a semi-infinite vertical flat plate in a porous medium, *Int. J. Heat Mass Transfer* **28,** 683–698 (1985).
5. T. W. Tong and E. Subramanian, A boundary layer analysis for natural convection in vertical porous enclosures—use of the Brinkman-extended Darcy model, *Int. J. Heat Mass Transfer* **28,** 563–572 (1985).
6. J. G. Georgiadis and I. Catton, Free convective motion in an infinite vertical porous slot: the non-Darcian regime, *Int. J. Heat Mass Transfer* **28,** 2389–2392 (1985).
7. J. G. Georgiadis and I. Catton, Prandtl number effect on Bénard convection in porous media, *ASME J. Heat Transfer* **108,** 284–289 (1986).
8. P. Forchheimer, Wasserbewegung durch boden, *Z. Ver. Dt. Ing.* **45,** 1782–1788 (1901).
9. H. C. Brinkman, A calculation of the viscous force exerted by a flowing fluid on a dense swarm of particles, *Appl. Scient. Res.* **1,** 23–34 (1947).
10. A. E. Gill, A proof that convection in a porous vertical slab is stable, *J. Fluid Mech.* **35,** 545–547 (1969).
11. V. P. Gupta and D. D. Joseph, Bounds for heat transport in a porous layer, *J. Fluid Mech.* **57,** 491–514 (1973).

Int. J. Heat Mass Transfer. Vol. 31, No. 7, pp. 1534–1537, 1988
Printed in Great Britain

0017–9310/88 $3.00 + 0.00

Surface tension driven flows for a droplet in a micro-gravity environment

D. L. R. Oliver and K. J. DeWitt
College of Engineering, University of Toledo, Toledo, OH 43606, U.S.A.

(*Received* 3 *August* 1987 *and in final form* 19 *January* 1988)

1. INTRODUCTION

With the advent of sustained space flight, studies related to chemical processes in a micro-gravity environment have become important. At low gravity fluid motion is often governed by forces which are often negligible in the earth's gravitational field. One of these forces which is expected to be important in a micro-gravity environment is surface tension. When a gradient in surface tension exists at the interface between two fluid phases, a surface tension driven (Marangoni) flow field may result. The surface tension between two fluids is a function of the temperature and the concentration level of any solute present at the fluid interface. Thus, in the presence of a gradient in the solute concentration or the temperature near a fluid interface, surface tension driven flows may be present. Surface tension (Marangoni) effects on droplets have been studied in several works including: Levan [1], Thompson *et al.* [2], and Rivkind and Sigovtsev [3].

The intent of this work is to demonstrate that irradiant

NOMENCLATURE

$a_i, a_{i,j}$ coefficients, equations (6) and (10)
$b_i, b_{i,j}$ coefficients, equations (7) and (11)
$C_n^{-1/2}(\cos\theta)$ Gegenbauer polynomials (see the appendix of Levan [1])
k thermal conductivity
K ratio of thermal conductivities, k_1/k_2
q'' thermal radiation flux
r dimensionless radius, R/R_0
R, R_0 radius and droplet radius, respectively
T temperature
u, v dimensionless radial and tangential velocities, $u = U/U_\infty$
U_∞ bulk droplet velocity, equation (20)
X ratio of dynamic viscosities, μ_1/μ_2.

Greek symbols
α absorptivity of the droplet surface
θ tangential coordinate
μ dynamic viscosity
σ surface tension
T dimensionless temperature, equation (1)
ψ dimensionless stream function, equations (23).

Subscripts
1 droplet phase
2 continuous phase
∞ free stream.

energy may be exploited to induce droplet motion in a micro-gravity environment. The analysis considers only the special case of an opaque droplet. This restriction is made to facilitate a straightforward closed form solution for the resulting flow field. In spite of this limitation, it is hoped that this work will enhance our understanding of how surface tension effects can be exploited in micro-gravity environments.

If the surface of the droplet acts as a diffuse gray body to a uniform irradiant energy source, the heat generation rate at the droplet surface will vary with the cosine of the tangential angle (Fig. 1). The resulting non-uniform heat generation rate at the droplet surface will create a temperature gradient near the droplet surface. This temperature gradient will in turn create a gradient in the surface tension along the droplet surface. In the absence of other forces such as gravity, the droplet will migrate slowly in a direction parallel to the incident radiation (generally towards the radiant energy source). It is the intent of this work to analytically estimate the flow field near such a droplet.

2. ANALYSIS

As with most analyses, several assumptions must be made to obtain a closed form solution. The continuous phase is assumed to be transparent to thermal radiation, while the droplet phase is assumed to be opaque to thermal radiation. This will result in generation of heat at the droplet surface that varies with the tangential angle. Since the surface tension is a function of the temperature, this non-uniform generation of heat at the droplet surface will create a gradient in the surface tension. For this investigation the surface tension is assumed to be a linear function of temperature only, and not a function of the concentration of any solutes present.

Surface tension driven flows near small droplets tend to be slow enough to justify the use of the creeping flow assumptions. For many fluids the Prandtl number is of the order of 1–100; thus for slowly moving droplets it is reasonable to assume that the heat transfer near the droplet will be due to conduction dominated heat transfer.

Specifically, the following assumptions are made in this analysis:

(1) the droplet is spherical and isolated in a quiescent fluid medium;
(2) the surface tension is a linear function of temperature only;
(3) constant fluid properties are assumed (except surface tension);
(4) the continuous phase is transparent to radiation;
(5) the droplet surface acts as a gray body;
(6) the incident irradiation is in the form of uniform parallel rays;
(7) the flow is axisymmetric;
(8) both the Reynolds number, and the product of the

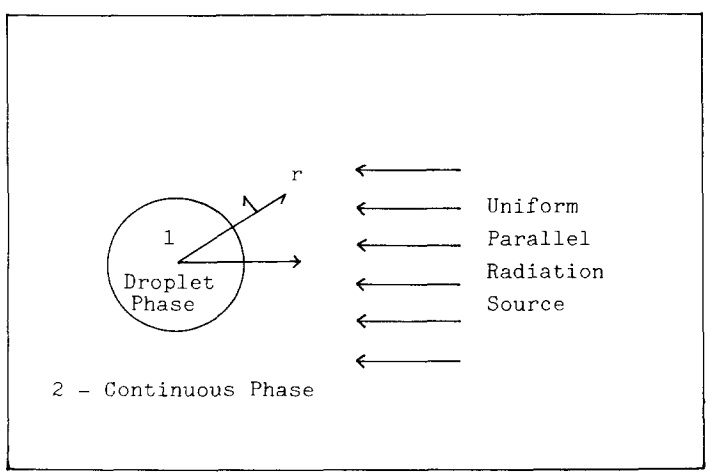

FIG. 1. Schematic of problem.

Reynolds number and the Prandtl number are small (i.e. $Re \ll 1$ and $Re\,Pr \ll 1$);

(9) a steady-state solution is sought.

The dimensionless equation for conduction in spherical coordinates is

$$\frac{\partial^2 T_i}{\partial r^2} + \frac{2}{r}\frac{\partial T_i}{\partial r} + \frac{1}{r^2 \sin\theta}\frac{\partial}{\partial \theta}\left(\sin\theta \frac{\partial T_i}{\partial \theta}\right) = 0 \quad (1)$$

where $K = k_1/k_2$ is the ratio of thermal conductivities, $r = R/R_0$ the dimensionless radius, and $T = k_2(T - T_\infty)/q''\alpha R_0$ the dimensionless temperature. The boundary conditions imposed on equation (1) are

$$T_1(r = 1, \theta) = T_2(r = 1, \theta) \quad (2)$$

$$-K\frac{\partial T_1}{\partial r} + \frac{\partial T_2}{\partial r} + \cos\theta = 0, \quad 0 < \theta < \pi/2, \quad r = 1 \quad (3a)$$

$$-K\frac{\partial T_1}{\partial r} + \frac{\partial T_2}{\partial r} = 0, \quad \pi/2 < \theta < \pi, \quad r = 1 \quad (3b)$$

$$\frac{\partial T_i}{\partial \theta} = 0, \quad \theta = 0, \pi \quad (4)$$

$$\lim_{r\to\infty} T_2(r, \theta) = 0. \quad (5)$$

Equation (1) with boundary conditions (2)–(5) is solved by introducing the following series:

$$T_1 = \sum_{i=0}^{\infty}\sum_{j=-\infty}^{\infty} a_{i,j} r^j P_i(\cos\theta), \quad 0 < r < 1 \quad (6)$$

$$T_2 = \sum_{i=0}^{\infty}\sum_{j=-\infty}^{\infty} b_{i,j} r^j P_i(\cos\theta), \quad r > 1 \quad (7)$$

where $P_i(\cos\theta)$ is the Legendre polynomial of order i, and $a_{i,j}$ and $b_{i,j}$ are coefficients which are to be determined.

With the use of certain properties of the Legendre polynomials [4], equation (1) becomes

$$a_{i,j}[j(j-1) + 2j - i(i+1)] = 0 \quad (8)$$

$$b_{i,j}[j(j-1) + 2j - i(i+1)] = 0. \quad (9)$$

Since the temperature at the droplet center is finite, only non-negative values of j have finite coefficients in equation (6); similarly (by equation (5)), only negative values of j have non-zero coefficients in equation (7). In addition, for a given value of i only two values for j will satisfy equations (8) and (9). Thus the series in equations (6) and (7) reduce to

$$T_1 = \sum_{i=0}^{\infty} a_i r^i P_i(\cos\theta), \quad \text{with } a_i = a_{i,i} \quad (10)$$

$$T_2 = \sum_{i=0}^{\infty} b_i r^{-(i+1)} P_i(\cos\theta), \quad \text{with } b_i = b_{i,-(i+1)}. \quad (11)$$

Equation (2) is thus reduced to

$$a_i = b_i \quad (12)$$

and equation (3) results in

$$a_i = [(K+1)i + 1]^{-1}\frac{(2i+1)}{2}\int_0^1 P_i(x)P_1(x)\,dx. \quad (13)$$

Coefficients a_i may then be shown to be

$$a_0 = 1/4 \quad (14)$$

$$a_1 = 1/[2(K+2)] \quad (15)$$

$$a_i = (-1)^{(i-2)/2}\frac{(2i+1)}{2[(K+1)i+1](i+2)(i-1)} \times \prod_{j=1}^{i/2}\left(\frac{2j-1}{2j}\right) \quad (\text{even}, i > 1)$$

$$a_i = 0 \quad (\text{odd}, i > 2). \quad (16)$$

Thus, the temperature along the fluid interface is given by

$$T(r = 1, \theta) = \sum_{i=0}^{\infty} a_i P_i(\cos\theta) \quad (17)$$

$$T(R = R_0, \theta) = T_\infty + \frac{q''\alpha R_0}{k_2}\sum_{i=0}^{\infty} a_i P_i(\cos\theta). \quad (18)$$

If the surface tension is assumed to be a linear function of the temperature, it follows that the surface tension (σ) along the interface is given by

$$\sigma = \sigma_\infty + \frac{\partial\sigma}{\partial T}\frac{q''\alpha R_0}{k_2}\sum_{i=0}^{\infty} a_i P_i(\cos\theta). \quad (19)$$

The flow field which results from this gradient in the surface tension may be obtained from equations (12)–(22) of Levan [1]. In the analysis of Levan [1], the equations of motion are solved for the special case of axisymmetric flow about a droplet with a variable interfacial surface tension. The resulting flow field is presented by Levan as an infinite series of Gegenbauer functions (see the appendix of Levan [1]), with corresponding radial functions. The flow field for the present problem may be readily obtained from Levan's work using the surface tension profile given by equation (19) of the present work.

From equations (18)–(22) of Levan the bulk velocity of the droplet due to surface tension effects may be estimated

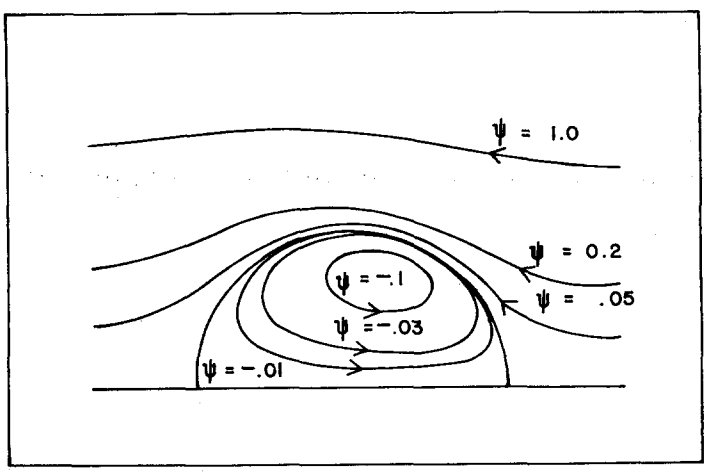

FIG. 2. Streamline contours: $X = 1$, $K = 1$.

to be

$$U_\infty = -\frac{\partial\sigma}{\partial T}\frac{q''\alpha R_0}{k_2}\frac{1}{3\mu_2}\frac{1}{(K+2)(2+3X)} \quad (20)$$

where μ_2 is the dynamic viscosity of the continuous phase, and X is the ratio of viscosities (droplet to continuous phase). The stream function values (made dimensionless by $U_\infty R_0^2$) are obtained from equations (12) and (13) of Levan

$$\psi_1 = \frac{-3}{4}(r^2-r^4)\sin^2\theta + \sum_{\substack{n=3\\(\text{odd})}}^{\infty}\frac{3n(n-1)(2+3X)(K+2)}{2(2n-1)(1+X)} \times a_{n-1}(r^{2+n}-r^n)C_n^{-1/2}(\cos\theta) \quad (21)$$

$$\psi_2 = (r^2-r^{-1})\frac{\sin^2\theta}{2} + \sum_{\substack{n=3\\(\text{odd})}}^{\infty}\frac{3n(n-1)(2+3X)(K+2)}{2(2n-1)(1+X)} \times a_{n-1}(r^{3-n}-r^{1-n})C_n^{-1/2}(\cos\theta) \quad (22)$$

with

$$u = \frac{-1}{r^2\sin\theta}\frac{\partial\psi}{\partial\theta}, \quad v = \frac{1}{r\sin\theta}\frac{\partial\psi}{\partial r}. \quad (23)$$

3. DISCUSSION

The bulk droplet velocity predicted by equation (20) is much smaller than that which would be significant in most buoyancy driven flows in the earth's gravitational field. However, surface tension driven velocities could be significant in a micro-gravity environment. The flow lines inside and near such a droplet are illustrated in Fig. 2, for the special case where the ratio of viscosities and thermal conductivities are unity (i.e. $X = 1$, $K = 1$).

Perhaps the most restrictive of the assumptions made in the preceding analysis is assumption (5), the assumption that the droplet surface acts as a gray body to the incident irradiant energy. Most droplets will be semi-transparent to irradiant energy in the visible range. Thus the preceding analysis is strictly valid for only a few systems. However, if the droplet absorbs a significant amount of the incident irradiant energy, the droplet will have a non-uniform temperature profile which can induce droplet motion resulting from gradients in the interfacial surface tension. The bulk droplet velocity for such a semi-transparent droplet is expected to be smaller, yet qualitatively similar to that predicted by equation (20).

REFERENCES

1. M. D. Levan, Motion of a droplet with a Newtonian interface, *J. Colloid Interface Sci.* **83**(3), 11–17 (1980).
2. R. L. Thompson, K. J. DeWitt and T. L. Labus, Marangoni bubble motion phenomenon in zero gravity, *Chem. Engng Commun.* **5**, 299–314 (1980).
3. V. Ya. Rivkind and G. S. Sigovtsev, Motion of a droplet in a nonisothermal flow, *Fluid Mech.—Sov. Res.* **10**(1), 36–46 (1981).
4. J. D. Talman, *Special Functions*, Chap. 9. W. A. Benjamin, Menlo Park, California (1968).

Int. J. Heat Mass Transfer. Vol. 31, No. 7, pp. 1537–1539, 1988
Printed in Great Britain

0017-9310/88 $3.00+0.00
Pergamon Press plc

Radiation configuration factors from axisymmetric bodies to plane surfaces

M. H. N. NARAGHI
Department of Mechanical Engineering, Manhattan College, Riverdale, NY 10471, U.S.A.

and

J. P. WARNA
Department of Chemical Engineering, University of Abo Akademi, Turku, Finland

(*Received* 28 *September* 1987 *and in final form* 19 *January* 1988)

INTRODUCTION

A LARGE number of view factors between a variety of surfaces has been evaluated using different numerical and analytical methods [1]. A close examination of the literature reveals that little work has been done on the view factors between axisymmetric bodies and plane surfaces. This note develops a general formulation for evaluating the view factors between axisymmetric bodies and plane surfaces perpendicular to the axis of symmetry.

FORMULATION

Consider the configuration shown in Fig. 1, consisting of an axisymmetric body and a plane surface perpendicular to the axis of symmetry. The view factor from differential areas to most commonly used axisymmetric bodies are known, e.g. the view factors from a differential area to a disk [2], a cylinder [3], a cone [4, 5], a sphere [6, 7] and a spherical segment [8].

A differential ring sector can be generated by rotating the differential area about the axis of symmetry as shown in Fig. 1. Note that the angle of rotation is ϕ. Thus, the view factor from the axisymmetric body to the planar surface can be determined by integrating the view factor from the axisymmetric body to the differential ring over the area of the planar surface

$$F_{Ax-A} = \int_{a_1}^{a_2} \mathrm{d}F_{Ax-\delta r} \quad (1)$$

where

$$\mathrm{d}F_{Ax-\delta r} = \phi\frac{\mathrm{d}F_{Ax-\mathrm{d}A}}{\mathrm{d}\phi} = \phi F_{\mathrm{d}A-Ax}\frac{\mathrm{d}A/\mathrm{d}\phi}{Ax} \quad (2)$$